

Non-aqueous Metal–Oxygen Batteries: Past, Present, and Future

Maxwell D. Radin and Donald J. Siegel

1 What Is the Motivation for High Energy-Density Batteries?

A metal-oxygen battery (sometimes referred to as a ‘metal-air’ battery) is a cell chemistry in which one of the reactants is gaseous oxygen, O_2 . Oxygen enters the cell typically in the positive electrode—perhaps after being separated from an inflow of air—and dissolves in the electrolyte. The negative electrode is typically a metal monolith or foil. Upon discharge, metal cations present in the electrolyte react with dissolved oxygen and electrons from the electrode to form a metal-oxide or metal-hydroxide discharge product. In some chemistries the discharge product remains dissolved in the electrolyte; in other systems it precipitates out of solution, forming a solid phase that grows in size as discharge proceeds. In secondary metal-oxygen batteries the recharge process proceeds via the decomposition of the discharge phase back to O_2 and dissolved metal cations. In light of the processes associated with discharge and charging, reversible metal-oxygen batteries with solid discharge products are often referred to as precipitation-dissolution systems, a category that also includes lithium–sulfur batteries.

The interest in metal-oxygen chemistries follows from their very high theoretical energy densities. Figure 1 summarizes the gravimetric and volumetric energy densities for several metal-oxygen couples, and compares these to the theoretical energy density of a conventional lithium-ion battery. On the basis of these energy densities, it is clear that many metal-oxygen systems hold promise for surpassing the state-of-the-art Li-ion system.

Achieving this goal, however, remains a significant challenge when factors beyond energy density are accounted for: cycle life, round-trip efficiency, and cost

M.D. Radin · D.J. Siegel (✉)
University of Michigan, Ann Arbor, USA
e-mail: djsiege@umich.edu

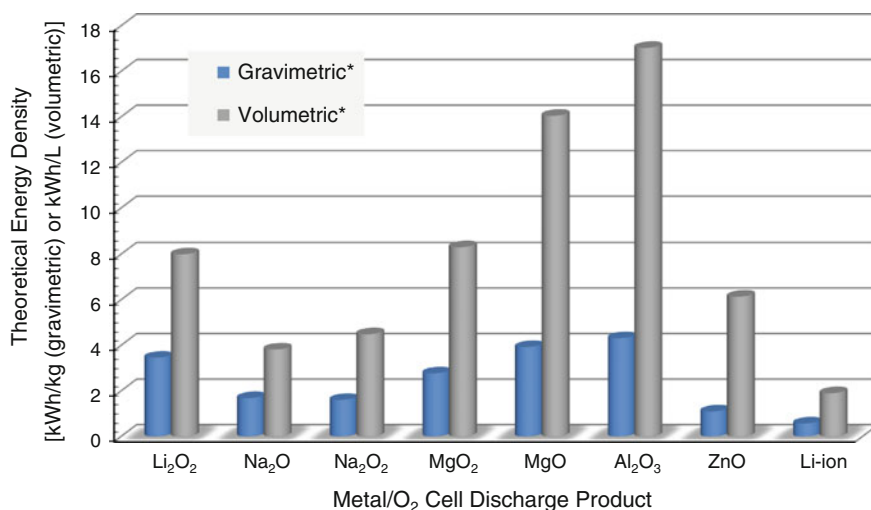


Fig. 1 Theoretical energy densities for several metal-oxygen couples compared to a conventional Li-ion battery. The abscissa indexes the discharge product(s) associated with each metal composition

must also be considered. The present chapter serves as a primer for new researchers interested in tackling these challenges. We begin with a brief history of metal-oxygen batteries, followed by a deep-dive into arguably the most ambitious secondary metal-oxygen chemistry, the non-aqueous Li-O₂ system. The current status of Li-O₂ cell performance is summarized with an emphasis on capacity, rate capability, cycle life, and efficiency. Subsequent sections review (i.) operating mechanisms, (ii.) challenges and failure modes, and (iii.) novel concepts for improving performance. We conclude with a brief discussion of non-lithium-based systems.

2 The History of Metal-Oxygen Batteries

2.1 Overview of Metal-Oxygen Batteries

The long history of metal-oxygen batteries is often unappreciated. To our knowledge, the earliest written description of a metal-oxygen battery is Vergnes' aqueous Zn-air battery from 1860 [1]. This design is in some respects remarkably similar to today's advanced metal-oxygen cells, which frequently employ porous carbon positive electrodes and noble-metal catalysts [2]. Figure 2 shows Vergnes' design, containing a zinc metal anode and a porous platinized coke positive electrode. The overall reaction in these cells is $\text{Zn} + \frac{1}{2}\text{O}_2 \rightarrow \text{ZnO}$. Zn-air batteries matured into a practical energy storage technology in the early 20th century [3], and as of the early

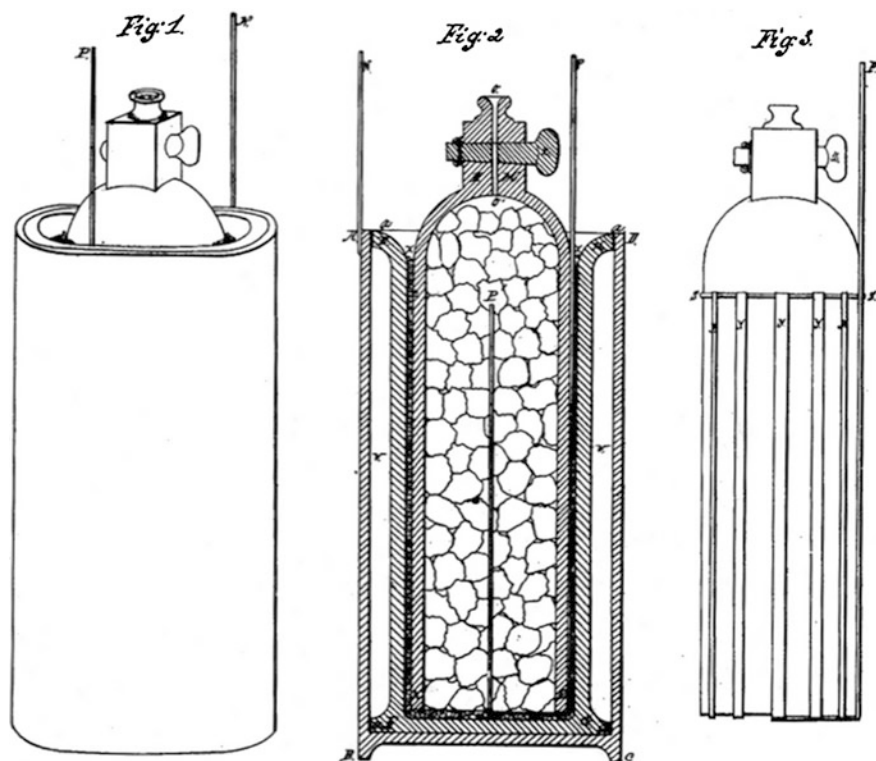


Fig. 2 Vergnes' 1860 Zn-air battery design, taken from Ref. [1]

21st century still remain the most prominent metal-oxygen chemistry. Industrially produced primary Zn-air cells exhibit high energy densities [4] and are employed in a number of applications, such as hearing aids.

Over the years, many other metal-oxygen couples have also been considered. In Tables 1 and 2, we enumerate reports of operating metal-oxygen cells, as well as oxygen cells based on the oxidation of several non-metals (C, H, and Si). The references cited in these tables are not intended to capture all of the work done on each metal-oxygen couple, but rather to highlight reviews and representative experiments. Table 1 shows cells that employ aqueous electrolytes, including composite electrolytes (i.e., the combination of a solid electrolyte in addition to an aqueous electrolyte). Table 2 shows non-aqueous chemistries, which are subdivided into high- and low-temperature. While all metal-oxygen chemistries can in principle be mechanically recharged (by replacing the metal anode and/or electrolyte), in Tables 1 and 2 we denote only those that are *electrochemically* rechargeable as 'secondary batteries.' Although Tables 1 and 2 are limited to couples in which a single element is oxidized, it should be noted that so-called 'direct' fuel cells involve the oxidation of compounds with multiple elements, including sugars [5], methanol [6], formic acid [7], and borohydrides [8].

Table 1 Summary of oxygen couples with aqueous electrolytes

	Reaction	Type of electrolyte	
		Non-composite	Composite
H	$\text{H}_2 + \frac{1}{2}\text{O}_2 \rightarrow \text{H}_2\text{O}$	Secondary [4, 6]	
Li	$\text{Li} + \frac{1}{4}\text{O}_2 + \frac{1}{2}\text{H}_2\text{O} \rightarrow \text{LiOH}$	Primary [11]	Secondary [15]
Na	$\text{Na} + \frac{1}{4}\text{O}_2 + \frac{1}{2}\text{H}_2\text{O} \rightarrow \text{NaOH}$		Primary [157]
Mg	$\text{Mg} + \frac{1}{2}\text{O}_2 + \text{H}_2\text{O} \rightarrow \text{Mg}(\text{OH})_2$	Primary [4, 158]	
Ca	Unknown	Primary [159]	
V	$4\text{H}^+ + \text{O}_2 + 4\text{V}^{2+} \rightarrow 2\text{H}_2\text{O} + 4\text{V}^{3+}$		Secondary [160]
Mo	$\text{Mo} + \frac{3}{2}\text{O}_2 + \text{H}_2\text{O} \rightarrow \text{H}_2\text{MoO}_4$	Primary [161]	
	$\text{Mo} + \frac{3}{2}\text{O}_2 + 2\text{KOH} \rightarrow \text{K}_2\text{MoO}_4 + \text{H}_2\text{O}$	Primary [161]	
Fe	$\text{Fe} + \frac{1}{2}\text{O}_2 + \text{H}_2\text{O} \rightarrow \text{Fe}(\text{OH})_2$	Secondary [4]	
	$3\text{Fe}(\text{OH})_2 + \frac{1}{2}\text{O}_2 + \text{H}_2\text{O} \rightarrow \text{Fe}_3\text{O}_4 + 4\text{H}_2\text{O}$	Secondary [4]	
Zn	$\text{Zn} + \frac{1}{2}\text{O}_2 \rightarrow \text{ZnO}$	Secondary [4]	
Cd	Unknown	Secondary [162]	
Al	$\text{Al} + \frac{3}{4}\text{O}_2 + \frac{3}{2}\text{H}_2\text{O} \rightarrow \text{Al}(\text{OH})_3$	Primary [4, 163]	Secondary [164]
Si	$\text{Si} + \text{O}_2 + 2\text{H}_2\text{O} \rightarrow \text{Si}(\text{OH})_4$	Primary [165]	
Sn	$\text{Sn} + \text{O}_2 + 2\text{KOH} + 2\text{H}_2\text{O} \rightarrow \text{K}_2\text{Sn}(\text{OH})_6$	Primary [166]	

Table 2 Summary of couples with non-aqueous electrolytes

	Reaction	Type of cell demonstrated	
		Low-temperature	High-temperature
H	$\text{H}_2 + \frac{1}{2}\text{O}_2 \rightarrow \text{H}_2\text{O}$	Secondary [6]	Secondary [6]
Li	$2\text{Li} + \text{O}_2 \rightarrow \text{Li}_2\text{O}_2$	Secondary [2, 15, 16]	
	$\text{FeSi}_2\text{Li}_x + \frac{3}{4}\text{O}_2 \rightarrow \frac{3}{2}\text{Li}_2\text{O} + \text{FeSi}_2$		Secondary [12]
Na	$\text{Na} + \text{O}_2 \rightarrow \text{NaO}_2$	Secondary [144, 145]	
	$2\text{Na} + \text{O}_2 \rightarrow \text{Na}_2\text{O}_2$	Secondary [145, 146]	
K	$\text{K} + \text{O}_2 \rightarrow \text{KO}_2$	Secondary [147]	
Mg	$\text{Mg} + \frac{1}{2}\text{O}_2 \rightarrow \text{MgO}$	Secondary [148]	Primary [167]
Ca	$2\text{CaSi} + \frac{1}{2}\text{O}_2 \rightarrow \text{CaO} + \text{CaSi}_2$		Secondary [168]
Mo	$\text{Mo} + \text{O}_2 \rightarrow \text{MoO}_2$		Secondary [169]
W	$\text{W} + \text{O}_2 \rightarrow \text{WO}_2$		Secondary [170]
Fe	$\text{Fe} + \frac{1}{2}\text{O}_2 \rightarrow \text{FeO}$		Secondary [171]
	$3\text{Fe} + 2\text{O}_2 \rightarrow \text{Fe}_3\text{O}_4$		
Al	Unknown	Secondary [150]	
C	$\text{C} + \text{O}_2 \rightarrow \text{CO}_2$		Primary [172]
Si	$\text{Si} + \text{O}_2 \rightarrow \text{SiO}_2$	Primary [173]	

Here ‘low-temperature’ refers to cells that operate below 100 °C and ‘high-temperature’ to those that operate above 100 °C

2.2 History of Li–O₂ Technology

The birth of the modern non-aqueous Li–O₂ battery is generally considered to be the 1996 demonstration of a room-temperature secondary cell by Abraham and Jiang [9]. While this development was a breakthrough, the history of earlier Li–O₂ batteries is often overlooked. To the best of our knowledge the first investigation of the Li–O₂ couple dates back to 1966 [10]. Although this early study also employed non-aqueous electrolytes—including propylene carbonate, today’s preeminent Li-ion solvent—the design pursued was a ‘moist’ Li–O₂ system: the oxygen supply was saturated with water vapor. Interestingly, even this preliminary study identified some of the issues that remain critical for modern Li–O₂ cells, such as the formation of lithium carbonate and the role of impurities.

Other Li–O₂ designs emerged later. Primary Li–O₂ cells with aqueous electrolytes received considerable attention in the 1970s [11], and moisture-free high-temperature secondary cells were developed in the 1980s [12]. However, Abraham and Jiang’s 1996 study represents the first demonstration of a moisture-free room temperature secondary Li–O₂ cell [9], and is therefore a key development in the history of Li–O₂ batteries. An amusing historical note is that the development of this cell was not intentional, but was instead a serendipitous discovery caused by the leakage of oxygen from a syringe into a sealed lithium-graphite cell [13].

Since 1996, research on non-aqueous Li–O₂ cells grown immensely. This has also led to the development of related chemistries, including true Li-air cells [14] (i.e., using ambient air rather than pure oxygen) and also reversible aqueous Li–O₂ cells [15]. It is not possible to summarize all of the studies performed to date. Instead, we strive to summarize and unify the key lessons, observations, and hypotheses that have been presented in the literature. For additional details beyond those presented here, the reader is encouraged to explore other reviews of the field [2, 15–20].

3 State of the Art

3.1 Current Status—Current, Capacity, Cycle Life, Efficiency

Much of the research on non-aqueous Li–O₂ batteries has focused on improving four critical aspects of performance: rate capability, capacity, voltaic efficiency, and cycle life. Some state-of-the-art Li–O₂ cells have been demonstrated to perform adequately with regard to these measures individually, but none have performed satisfactorily in all four simultaneously. This is because rate capability, capacity, voltaic efficiency, and cycle life are highly interdependent, often in surprising ways. Some interdependencies manifest as tradeoffs in performance; examples include:

1. Higher discharge rates reduce maximum capacity due to electrical passivation issues and/or oxygen transport limitations, as discussed in Sects. 3.3.1 and 3.3.2.

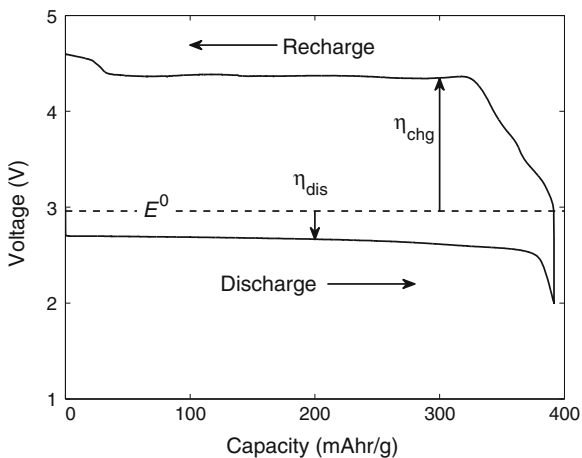


Fig. 3 Potential profile from a galvanostatic discharge/charge cycle of a parallel-electrode, aprotic Li–O₂ battery with a porous carbon positive electrode, Li metal anode, and LiTFSI/DME electrolyte at a current of 0.2 mA/cm². Data courtesy of L. Griffith, Monroe Research Group

2. Curtailing the discharge capacity increases cycle life and voltaic efficiency [21, 22].
3. Higher discharge rates (at fixed capacity) may *improve* voltaic efficiency, as the discharge product morphologies produced at high currents can exhibit lower charging overpotentials than the morphologies produced at low currents [23].

Figure 3 shows the potential profile from a galvanostatic discharge/charge cycle of a typical non-aqueous Li–O₂ cell. Several features shown here are typical for Li–O₂ cells. First, discharge proceeds at a constant voltage close to the theoretical cell potential E^0 for the formation of Li₂O₂. Discharge then terminates with a rapid drop in potential (‘sudden death’), possibly due to oxygen transport limitations or electrical passivation. The recharge potential profile is more complex and exhibits several distinct stages with high recharge overpotential η_{chg} , resulting in low voltaic efficiencies.

We next summarize the performance of state-of-the-art Li–O₂ cells and compare to performance targets. We note that comparing capacities and currents across different experiments is non-trivial because different authors adopt different normalization schemes [24, 25]. For example, many studies employing carbon-black electrodes report capacities normalized to the mass of the carbon black. Underlying this convention is the notion that the capacity ought to be proportional to the mass of the carbon black. This can lead to misleading conclusions in cases where the gas diffusion layer (GDL) or current collector contributes significantly to capacity; one study found that carbon-black mass normalization can inflate the capacity of a typical Li–O₂ electrode by as much as an order of magnitude [24]. The carbon-mass-normalization convention can also lead to misleading conclusions in cases where only a small fraction of the carbon black is utilized due to oxygen

transport limitations, as discussed in Sect. 3.3.2. Furthermore, this convention does not allow for meaningful comparison between electrodes where the mass of the catalyst and binder is significant, or to carbon-free electrodes.

To facilitate meaningful comparisons between experiments and with performance targets, we recommend the following protocol for reporting currents and capacities:

1. Capacities and currents should be reported normalized both to the mass and to the positive electrode's geometric area, because battery pack performance depends both on the current/capacity per mass and per geometric area. (At a minimum, one should supply enough data to allow readers to convert between normalization schemes.)
2. When normalizing to mass, the masses of all positive electrode components that scale with the loading (e.g., binders and catalysts) should be included because these contributions to the total mass are important from the perspective of battery system design.
3. If one excludes the mass of the GDL/current collector from the mass normalization, then one must verify that its contribution to capacity (per area or per cell) is negligible compared to the contribution from the active materials [23, 24]. Note that it is not sufficient to show that the capacity per mass of the GDL is small compared to the capacity per mass of the active material, because the mass of the GDL often greatly exceeds that of the active material.

The tradeoff between current and capacity is illustrated in Fig. 4, which shows the capacities and rates obtained in various Li–O₂ cells reported in the literature, normalized to the geometric area of the electrode. Additionally, the current densities

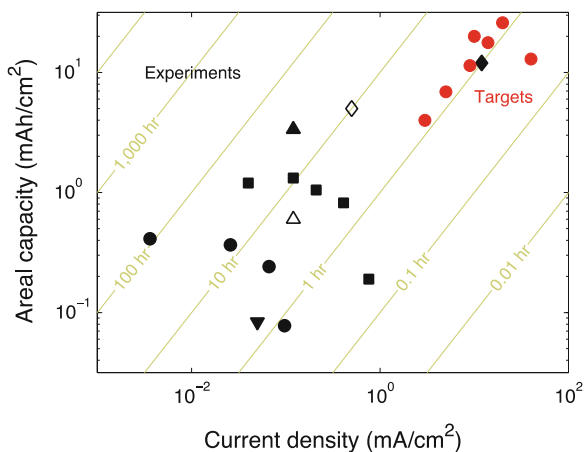


Fig. 4 Reported capacities for galvanostatic operation of Li–O₂ cells from various experiments [28, 29, 34, 155, 156] during the first discharge (*black solid symbols*) and in cells which can be cycled many times (*black open symbols*). The *red symbols* indicate the currents and capacities assumed in hypothetical battery designs [15, 26, 27]. *Diagonal lines* identify the time required for discharge (Color figure online)

and capacities assumed in several hypothetical designs for practical Li–O₂ batteries [15, 26, 27] are shown.

One of the fundamental reasons why current cell designs fall short of the areal performance targets [15, 26, 27] is electrode thickness: while experiments often consider electrodes of thickness $\sim 10\ \mu\text{m}$, proposed battery designs have assumed much larger thicknesses of 150–300 μm . A practical Li–O₂ battery requires that the electrode be fairly thick so as to minimize the mass and volume penalties associated with the inactive components (e.g., separators, electrolyte, current collectors, packaging). However, the full utilization of thick electrodes is likely limited by oxygen transport, as discussed in Sect. 3.3.2. Thus the development of a practical Li–O₂ battery will require either a solution to the oxygen transport problem within thick electrodes, or a battery pack design that achieves high system-level performance with thin electrodes.

The gap between experiments and targets is smaller on a mass basis. The mass-specific capacity targets of $\sim 1000\ \text{mAh/g}$ (including the mass of catalysts and binders) [26, 27] are routinely achieved at fairly high rates ($\sim 1\ \text{h}$ discharge), sometimes even over many cycles [28]. Although mass-capacities significantly higher than this have been reported [29, 30], from the perspective of system design there is limited benefit to increasing the gravimetric capacity beyond $\sim 1000\ \text{mAh/g}$. As the capacity increases beyond this value, the gravimetric capacity ultimately becomes limited by the mass of the discharge product [27]: the theoretical capacity of the Li–O₂ couple is $1168\ \text{mAh/g}_{\text{Li}_2\text{O}_2}$ [31].

In the next section, we summarize the key observations and theories regarding the operating mechanisms of Li–O₂ cells. Possible origins of these performance limitations are also described. It is important to keep in mind that different mechanisms may dominate under different operating conditions. For example, it has been shown that the current density [23], positive electrode material/architecture [32, 33], and system cleanliness [34–36] can play a significant role in the reaction mechanisms.

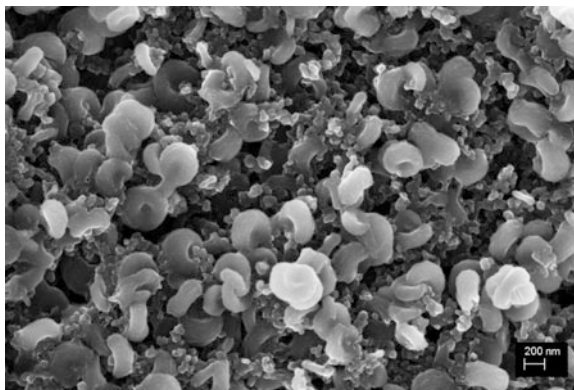
3.2 Proposed Mechanisms

3.2.1 The Discharge Product

The first step in understanding the performance of Li–O₂ batteries is understanding the discharge product. It is often presumed that the discharge product is bulk crystalline Li₂O₂; however, this is probably too simplistic an assumption, as there is now good evidence that the discharge product can have a complex morphology, microstructure, and composition.

Morphology. A number of different discharge product morphologies have been reported, including disks [23, 37], films [37, 38], needles [39], and hollow spheres [40]. Biconcave disks (similar to red blood cells) are among the most commonly observed morphologies, as shown in Fig. 5. (This morphology is often referred to as a ‘toroid’; however, these particles are not strictly speaking toroids because they

Fig. 5 SEM image of biconcave Li_2O_2 disks in a $\text{Li}-\text{O}_2$ cell. From Adams et al. [23]



lack a hole that runs through the center of the disk.) Figure 6 shows the basic structure of a typical Li_2O_2 disk, which consists of a stack of relatively flat crystallites. The disks are highly textured (i.e., the misorientation between crystallites is small), with the $\{0001\}$ axis being aligned with the central axis of the disk. In some cases the regions between the plates appear to be filled with components of the electrolyte [36], but in others it has been suggested that the inter-plate regions contain a distinct phase or grain boundary region [41]. This second phase could be, for example, amorphous Li_2O_2 or a lithium-deficient compound such as $\text{Li}_{2-x}\text{O}_2$. Note that it can be the case that multiple distinct morphologies appear concurrently in the positive electrode of a single cell; for example, large biconcave disks and small particles have been observed simultaneously [37].

The morphology of the discharge product has been suggested to influence discharge capacity and recharge overpotentials [23, 42–44]; therefore an understanding of the factors which control morphology may enable the design of cells with improved performance. It has been reported that low current densities and high water concentrations (hundreds to thousands of ppm) both promote the growth of biconcave disks [23, 37, 45–47]. Similar biconcave disks have also been observed in the precipitation of silicates [48] and corn starch [49], suggesting that there may be a common growth mechanism. It has also been reported that the characteristic size of these particles decreases with increasing current densities, and that at sufficiently high rates the deposit forms a conformal film rather than discrete particles [23, 37, 45, 47]. However, it has been suggested that the putative conformal films produced at high currents are in fact carpets of nano-scale needles [39]. Additionally, several experiments have concluded that the support and/or catalyst can strongly influence discharge product morphology [42–44].

A concrete picture of the discharge product growth mechanism remains elusive. A continuum-scale growth model has been proposed to explain the transition from particle to film with increasing current [50], and a separate model has been proposed to explain the increase in disk size with increasing water concentration [36].

Crystallinity. A growing number of experiments have suggested that amorphous Li_2O_2 can be present in the discharge product [23, 32, 33, 40]. The formation of an

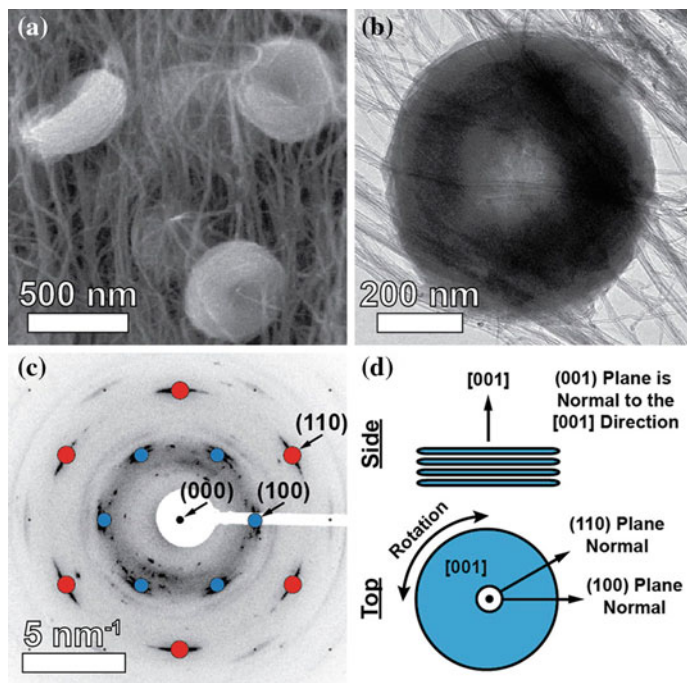


Fig. 6 Morphology of a biconcave $\text{Li}_2\text{-O}_2$ disk on a carbon nanotube support: **a** SEM, **b** bright-field TEM, **c** electron diffraction pattern, **d** schematic of microstructure. From Mitchell et al. [37]

amorphous deposit is consistent with Ostwald's rule, which states that unstable phases tend to precipitate before stable phases [51–53]. It has been reported that higher discharge rates [23], as well as certain catalysts, can promote the formation of amorphous Li_2O_2 [32, 33].

Several experimental [23, 32, 33] and computational [32, 54] studies have suggested that amorphous Li_2O_2 is easier to recharge than crystalline Li_2O_2 , perhaps due to improved electron or Li-ion transport properties. If correct, this would suggest that Li-O_2 electrode designs (or operating conditions) that promote the formation of amorphous Li_2O_2 may yield superior performance.

Composition. Although the discharge product is primarily thought of as Li_2O_2 , deviations from this composition have been proposed. One recurring theme is the occurrence of superoxide ions, O_2^- , in the discharge product [55]. The presence of a superoxide component perhaps should not be a surprise, given that it is known that other alkali metals form mixed peroxide-superoxide phases [56]. It remains unclear where exactly the superoxide component resides in the discharge product. It has been suggested to represent a surface species [57, 58], an oxygen-rich phase located in the inter-plate regions [41], or to be associated with the presence of point defects such as hole polarons [59, 60].

Relatively few studies have found evidence for Li_2O in the discharge product [61, 62]. Although Li_2O has a higher theoretical specific energy density than Li_2O_2 (5200 vs. 3505 Wh/kg [61]), it may not be a desirable discharge product for secondary Li– O_2 batteries because the electrochemical oxidation of Li_2O is more difficult than that of Li_2O_2 [63, 64].

It has been recognized that Li–O compounds are not the only phases present in the discharge product. Side reactions (i.e., reactions involving decomposition of the salt, solvent, or positive electrode) have been observed to produce other compounds, such as lithium carbonate, lithium acetate, lithium formate, and lithium fluoride [65, 66]. The products of these side reactions can comprise a substantial fraction of the discharge product; one experiment found that in a typical Li– O_2 cell with an ethereal solvent, the yield of Li_2O_2 was at best 91 % of the theoretical amount expected from coulometry [65]. It is important to note that in addition to the precipitated side reaction products, there may be additional soluble side reaction products. Side reactions are discussed in more detail in Sect. 3.3.4.

3.2.2 Discharge/Recharge Mechanisms

A number of different discharge and recharge mechanisms have been proposed, as illustrated in Fig. 7. It is important to keep in mind that different mechanisms may predominate depending on the experimental conditions (e.g., rate, electrolyte, electrode/catalyst, temperature, depth of discharge, and cleanliness).

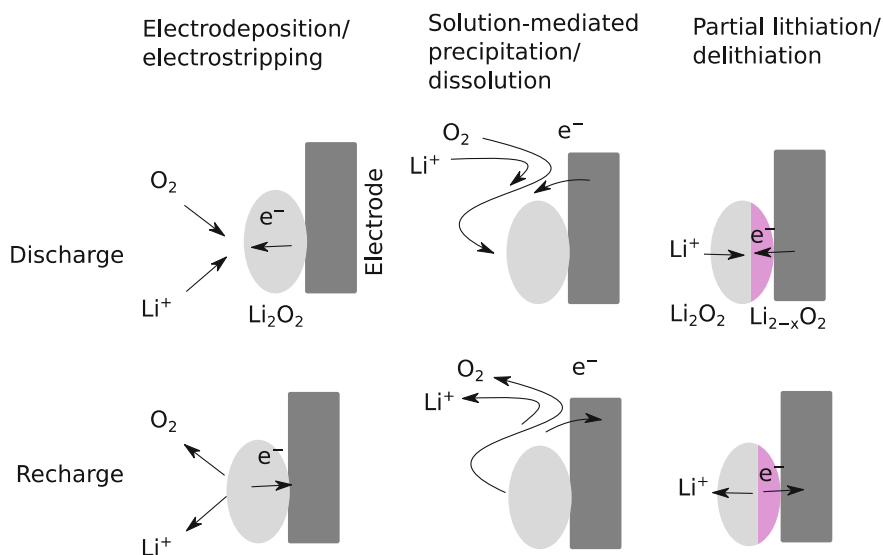


Fig. 7 Possible mechanisms for discharge/recharge in a Li– O_2 cell. As discussed in the text, in the case of solution-mediated mechanisms, there are many possible intermediate species; the central column illustrates a scenario where the intermediate species is molecular Li_2O_2

Electrodeposition/electrostripping. In some experiments it has been suggested that the growth/dissolution of a film occurs via the electrochemical deposition/stripping of Li_2O_2 . In such a mechanism, electron transport presumably would occur through the growing deposit. It has been suggested that this could occur via electron tunneling [38, 67] or hole polaron hopping [59, 60, 68]. Limitations associated with charge transport are discussed in Sect. 3.3.1.

Solution-mediated precipitation/dissolution. The growth of large particles has been proposed to occur via a solution-mediated precipitation process, which would allow charge-transport limitations through the particles to be bypassed [23, 69–71]. For example, one proposed discharge mechanism is that O_2 is reduced on the positive electrode surface to form LiO_2 : $\text{Li}^+ + \text{O}_2 + \text{e}^- \rightarrow \text{LiO}_2$. The LiO_2 could then diffuse in the electrolyte (or perhaps along the positive electrode surface), and then precipitate out via a disproportionation reaction: $2\text{LiO}_2 \rightarrow \text{Li}_2\text{O}_2 + \text{O}_2$. Such a mechanism requires that there be an intermediate species (be it LiO_2 or something else) that is either at least sparingly soluble or capable of rapid surface diffusion. Additives which solubilize such intermediates have been suggested to play a role in the dynamics of discharge product precipitation [46, 47].

A solution-mediated process (such as the reverse of the above reactions) could also occur during recharge. For example, it has been proposed that impurities present as contaminants or by-products of electrolyte decomposition may serve as the soluble intermediate species [35]. These impurities in effect function as redox mediators, or perhaps transform Li_2O_2 into a more soluble species. For example, a small amount of protons has been suggested to enable a recharge mechanism that begins with the transformation of Li_2O_2 into H_2O_2 via a single-displacement reaction, $\text{Li}_2\text{O}_2 + 2\text{H}^+ \rightarrow \text{H}_2\text{O}_2 + 2\text{Li}^+$ [35]. H_2O_2 , being more soluble than Li_2O_2 , could then diffuse to the electrode and be electrochemically oxidized via the reaction $\text{H}_2\text{O}_2 \rightarrow 2\text{H}^+ + \text{O}_2 + 2\text{e}^-$, yielding a net reaction of $\text{Li}_2\text{O}_2 \rightarrow 2\text{Li}^+ + \text{O}_2 + 2\text{e}^-$.

Partial lithiation/delithiation. The partial delithiation of the discharge product has been suggested to be the first step of recharge [60, 72–74]. This could occur as a two-phase reaction [72, 74]: $\text{Li}_2\text{O}_2 \rightarrow \text{Li}_{2-x}\text{O}_2 + x\text{Li}^+ + xe^-$. The equilibrium potential for this reaction when $x = 1$ has been calculated from first-principles methods to be 0.3–0.4 V above the equilibrium potential for the full oxidation of Li_2O_2 , $\text{Li}_2\text{O}_2 \rightarrow \text{O}_2 + 2\text{Li}^+ + 2\text{e}^-$ [72]. Partial lithiation/delithiation could also occur as a solid solution [60, 73]. Although the two-phase pathway is predicted to be thermodynamically more stable than the solid-solution pathway [72], the fact that high currents and small particle sizes can suppress phase separation in Li-ion battery materials [75] suggests that one cannot rule out the solid-solution pathway for Li– O_2 based on thermodynamics alone. Note that even if a delithiation process occurs (either via a two-phase or solid-solution pathway), the intermediate lithium-deficient phase may not be readily observable if recharge occurs one particle at a time (i.e., via a ‘domino cascade’ mechanism) [75].

3.3 Challenges/Failure Modes

3.3.1 Charge Transport Within the Discharge Product

Charge transport through the discharge product has been thought to limit the performance of Li–O₂ cells in many circumstances [38, 76–79]. The presence of a passivating layer on the positive electrode would shut down electrochemical activity, potentially leading to limitations in capacity, voltaic efficiency, and rate capability. Although the charge-transport mechanism(s) at play are not well understood, several possibilities have been proposed:

1. *Electron tunneling.* In thin films (<5 nm), electron tunneling has been suggested to be the dominant charge-transport mechanism [38, 67]. This mechanism has been suggested to account for sudden death behavior, which would occur when the film thickness exceeds the distance over which electron tunneling can readily occur.
2. *Hole polaron hopping.* Experiments and first-principles modeling have found that hole polarons are the dominant electronic charge carrier in Li₂O₂ [59, 60, 80]. Polaron hopping has also been suggested to account for sudden death behavior. In this scenario, sudden death would occur when the deposit thickness exceeds the thickness of space-charge layers associated with the Li₂O₂/electrolyte and Li₂O₂/electrode interfaces [81].
3. *Li-ion vacancy diffusion.* Experiments and first-principles modeling have found that Li-ion vacancies are the dominant Li defect in Li₂O₂ [60, 80]. The role of Li-ion vacancies is different from that of electronic charge carriers because ionic defects cannot readily cross the interface between the discharge product and electrode support [74]. That is, at the Li–O₂ equilibrium potential, the amount of Li which can be inserted into (or deinserted from) the positive electrode support typically represents only a small fraction of the amount of Li in the discharge product. Thus the support can be thought of as an ion-blocking electrode.

The relative importance of these mechanisms may vary depending on the conditions (discharge product morphology, temperature, current density, etc.). For example, some studies have speculated that charge transport in Li₂O₂ could be enhanced at extended defects, such as surfaces [57, 58, 82], grain boundaries [83], amorphous regions [32, 54], or interfaces [81, 84].

3.3.2 Oxygen Transport in the Electrolyte

In many cell designs the low solubility and diffusivity of oxygen in the electrolyte can limit discharge capacity [25, 76, 85–89]. In this case, only the region of the positive electrode near the gas inlet is utilized. Sluggish oxygen transport can be further compounded by pore-clogging, i.e., the obstruction of oxygen-diffusion pathways by the discharge product [87]. Oxygen transport limitations can lead to a sudden drop in voltage during a galvanostatic discharge (sudden death) [87–89].

Improvements in oxygen transport may be required in order to fully utilize the thick electrodes required to meet performance targets, as discussed in Sect. 3.1. While tailoring the pore network of the electrode (as discussed in Sect. 3.4.1) can improve oxygen transport, it cannot overcome the fundamental limits determined by the solubility and diffusivity (i.e., permeability) of oxygen in the electrolyte [88]. Strategies for extending these fundamental limits are discussed in Sect. 3.4.5.

3.3.3 Kinetics

A number of studies have examined the kinetics of Li–O₂ cells. Systematic experiments have found that both the discharge and recharge kinetics are facile [79]. Several computational studies have explored mechanisms for the layer-by-layer deposition/stripping of Li₂O₂. The ‘thermodynamic overpotentials’ associated with layer-by-layer deposition/stripping were found to be small (<0.2 V), and it was suggested on this basis that kinetics would be fast [90]. (Note, however, that thermodynamic overpotentials can only be compared qualitatively to the overpotentials observed in experiments; for example, the thermodynamic overpotentials do not account for the density of reactive sites (e.g., step edges or kinks) or the exchange currents associated with different reaction steps.) A few other first-principles studies concluded that the kinetics of layer-by-layer deposition/stripping was slow, and would limit cell performance [91, 92]. The differences among conclusions in the literature result primarily not from differences among atomistic calculations, but rather from differing interpretations of the computational results—that is, how the energies for various reaction steps relate to the current-voltage relationship.

3.3.4 Degradation

Most experiments on Li–O₂ systems prior to 2010 used electrolytes developed for Li-ion batteries, employing carbonate solvents such as propylene carbonate (PC), ethylene carbonate (EC), and dimethyl carbonate (DMC). These solvents were natural choices, as they had been widely successful for Li-ion batteries; some even refer to PC as ‘the new water’ due to its widespread use for Li-ion electrochemistry [93]. In 2010 the Li–O₂ community began to recognize that carbonate solvents are in fact highly unstable in Li–O₂ cells [94–96]. Therefore, studies prior to 2010 must be regarded with caution, since electrolyte degradation, rather than Li–O electrochemistry, is thought to dominate carbonate-containing Li–O₂ cells.

It is now recognized that solvent stability is a critical issue for Li–O₂ batteries [2, 15, 97], and furthermore it has been observed that the salt [98–100], carbon support [101, 102], and binder [103] can also react irreversibly. Side reactions can lead to poor cyclability due to the loss of electrolyte and accumulation of side-reaction products [97, 102, 104]. Furthermore, the oxidation of side-reaction products during recharge can result in high charging overpotentials [101, 102].

Quantitative measurements [e.g., via differential electrochemical mass spectroscopy (DEMS)] are critical for distinguishing reversible cycling from parasitic processes [97]. This is demonstrated in Fig. 8, which shows the cycling of a typical Li–O₂ cell. Figure 8a shows that the cell is cyclable; in fact the capacity increases during the first few cycles. However, the cycling does not represent the reversible formation of Li₂O₂. Figure 8b and c show that the amount of oxygen released during discharge is less than the amount consumed during discharge. Furthermore, Fig. 8d shows that the ratio of electrons transferred to oxygen released during recharge deviates dramatically from the value which would be expected for the oxidation of Li₂O₂, 2e⁻/O₂. Thus despite the apparent cycability of this cell, the chemistry is dominated by side reactions.

Much work presently is being done to design Li–O₂ cells with sufficient stability for a practical battery. The stability of the solvent, salt, and support/catalyst are interdependent [102, 105]; thus the challenge is to find a combination of these that are sufficiently stable. Carbonate solvents have been abandoned in favor of ethers, ionic liquids, and other solvent classes [19, 106]. Although an improvement over carbonates, even these solvents exhibit some degree of degradation [65, 66]. For example, a typical ethereal electrolyte with a carbon positive electrode was found to exhibit an Li₂O₂ yield of at most 91 % [65]. Improved stability has been reported for certain combinations, such as LiClO₄/DMSO with a nanoporous gold positive electrode [105].

Since the number of possible salt/solvent/electrode combinations is large, a mechanistic understanding of degradation processes will be important for

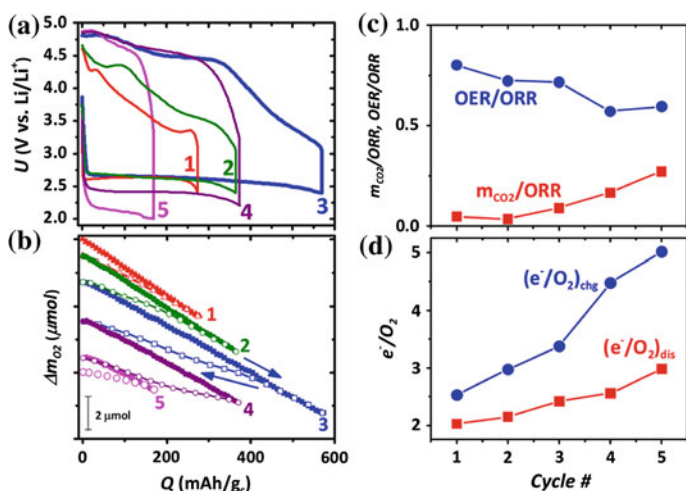


Fig. 8 **a** Potential profiles for five discharge/charge cycles of a Li–O₂ cell with Li-TFSI/DME electrolyte. **b** Oxygen consumption/evolution during discharge/charge. **c** Ratio of the amount of oxygen and CO₂ released during charge to the amount of oxygen consumed during discharge. **d** Ratio of the number of electrons transferred at the positive electrode to number of oxygen molecules consumed/evolved during discharge/charge. From McCloskey et al. [97]

identifying combinations with high stability. A summary of some of the solvent degradation processes that have been proposed is presented below. (Less effort has been invested in a mechanistic understanding of salt [99, 107], support, and binder stability, although these are clearly critical issues.)

1. *Chemical attack by electrochemical intermediates.* Chemical attack by intermediates of the oxygen reduction reaction during discharge can cause substantial degradation in some solvents. In particular, attack by superoxide (O_2^-) radicals is thought to be the main source of decomposition in carbonate solvents [108]. Others have suggested that oxidation intermediates could also lead to solvent degradation during recharge. In particular, ‘nascent’ oxygen evolved during recharge has been speculated to attack the solvent [97, 109]. Here ‘nascent’ refers to oxygen released in a highly reactive form, such as atomic oxygen or O_2 molecules in the singlet state.
2. *Auto-oxidation.* Organic solvents can undergo auto-oxidation (chemical reaction with molecular O_2). This has been hypothesized to contribute to solvent degradation in Li-O_2 cells [110, 111]. The importance of auto-oxidation may not be visible in typical experiments, whose time scales (days) are much shorter than those required for a practical automotive battery (years).
3. *Chemical attack by the discharge product.* Another solvent degradation mechanism is the chemical reaction between the solvent and the discharge product. A few experiments have sought to probe this [97, 100], and atomistic studies have examined solvent degradation on Li_2O_2 clusters [112] and surfaces [113].
4. *Electrochemical oxidation.* In addition to the chemical degradation processes listed above, electrochemical processes can also lead to solvent degradation. Many common solvents exhibit minimal oxidation up to ~ 4 V versus Li/Li^+ on carbon electrodes. However, it has been suggested that solvent oxidation is enhanced by Li_2O_2 [97]. Additionally, some oxygen-reduction catalysts used in Li-O_2 cells also catalyze solvent oxidation [114, 115].

3.3.5 Impurities

The presence of even small amounts of impurities have been suggested to have a substantial effect on cell performance [34, 35, 46, 47, 116–118]. We focus on H_2O , as this appears to be the most problematic and well-documented contaminant. It has been observed that even small amounts of water can influence Li-O_2 cells in complex ways:

1. The presence of water at concentrations as low as a few hundred ppm can significantly increase discharge capacity [21, 34, 47, 116].
2. Water can influence the discharge product morphology [21, 46, 47], and it has been found that concentrations of water in the hundreds to thousands of ppm can promote the formation of biconcave disks; see Sect. 3.2.1.

3. Water can significantly reduce the cyclability of Li–O₂ cell [21, 116].
4. The presence of water can result in the formation of LiOH, instead of, or in addition to, Li₂O₂ [14, 21].

The mechanisms by which water interacts with cell operation are not well understood. Water can react with Li metal in the negative electrode, as discussed in Sect. 3.3.6 [116]. Furthermore, water has been suggested to act as a mediator or solubilizing agent during discharge and/or recharge [35, 46, 47], as discussed in Sect. 3.2.2.

The minimization of water contamination in a Li–O₂ cell is non-trivial task [116], and it may be impractical to reduce the water concentration below ~ 10 ppm. However, it is not clear whether the complete elimination of water is necessary, or even desirable, for a practical Li–O₂ battery [46].

The effects of contamination by CO₂ have also been explored. It has been observed that CO₂ will react with the discharge product to form Li₂CO₃ [118]. Because of the high potentials required to oxidize Li₂CO₃ (and accompanying electrolyte decomposition), exposure to CO₂ should be minimized in secondary Li–O₂ cells. Unsaturated oxygenated hydrocarbons present as impurities in industrially produced ethers have also been found to be reactive in Li–O₂ cells [117].

3.3.6 Negative Electrode

Although graphite is the negative electrode of choice for commercial Li-ion batteries, the full benefit of the high specific capacity of the Li–O₂ positive electrode can only be realized when it is paired with a high specific capacity negative electrode. For this reason, nearly all Li–O₂ experiments to date have employed Li-metal negative electrodes [119]. Consequently, we focus in the remainder of this section of Li-metal negative electrodes. Of course, practical Li–O₂ cells could also take advantage of alternative negative electrodes, such as Si alloys [119].

We can divide challenges for Li-metal negative electrodes in Li–O₂ batteries into two categories: (i) challenges that are intrinsic to Li-metal electrodes (and which arise regardless of what positive electrode is used), and (ii) challenges that are specific to Li–O₂ systems. Among the intrinsic challenges for Li-metal electrodes, dendrite formation and coulombic efficiency are perhaps the most prominent. Intrinsic challenges for Li-metal electrodes will not be discussed here, as these have been reviewed elsewhere [4, 120].

Regarding challenges that are specific to Li–O₂ batteries, it has been recognized that the crossover of molecular oxygen, contaminants, and/or soluble side reaction products from the positive electrode may have a deleterious effect [116, 121, 122]; however, one study found that the presence of O₂ can promote the formation of a stable solid-electrolyte interphase (SEI) in DMSO [123]. The high reactivity of Li metal may require that the negative electrode of a practical Li–O₂ battery be protected with a solid electrolyte or SEI.

Note that most Li–O₂ experiments do not distinguish between limitations of the positive and negative electrodes, and in some cases it has been found that the Li-metal negative electrode contributes significantly to cyclability limitations and cell impedance [116, 124, 125]. A few studies have used Li_xFePO₄ instead of Li metal [126, 127]. This configuration would not be used in a practical battery because the equilibrium potential for the lithiation of Li_xFePO₄ is above the equilibrium Li–O₂ potential; however, the use of a highly stable electrode such as Li_xFePO₄ can allow one to isolate the phenomena specific to the O₂ electrode [126, 127].

3.4 Novel Concepts

Numerous new designs and materials have been developed in the years since Abraham and Jiang's development of the modern non-aqueous Li–O₂ battery. It is not possible to discuss them all here; rather we highlight a few novel concepts.

3.4.1 Advanced Positive Electrodes

While a 'baseline' Li–O₂ positive electrode consists of carbon black and binder, gains in performance have been reported using more advanced designs. Many studies have sought to modify the structure of the carbon at the nano-, micro-, or macro-scale [17, 18, 128]. Some experiments have explored carbon-free electrodes. Nanoporous gold [105] and titanium carbide [126] electrodes with DMSO-based electrolytes have been shown to have improved performance over carbon electrodes. The addition of new materials such as oxides and transition metals [2, 17, 18] has also been examined. These additions are frequently referred to as 'catalysts', but this terminology is misleading given these materials most likely do not function as conventional electrocatalysts. The term 'promoter' has been suggested as a more general term to describe materials which improve performance [42, 129].

3.4.2 Redox Mediators

The use of redox mediators has been shown to reduce charging overpotentials, presumably by bypassing charge transport limitations in the discharge product [127, 130]. The idea is that a soluble species that undergoes a reversible redox reaction at a potential near the Li–O₂ redox potential would be able to ferry electrons from the electrode to the discharge product. This mechanism assumes facile charge transfer from the mediator to the electrode. Such a mechanism may be incompatible with achieving high capacities: electron transfer will be blocked if the (insulating) discharge product covers the cathode support.

3.4.3 All Solid-State Designs

A somewhat different approach to the Li–O₂ chemistry is the all solid-state design. In this case the positive electrode is a porous material with the ability to support both lithium-ion and electron transport. Lithium and oxygen would react to form solid Li₂O₂ or Li₂O in the pores. Solid-state Li–O₂ cells have been demonstrated using composite cathodes comprised of carbon and LAGP, a fast ion conductor [15, 131]. Potential advantages of a solid-state design include improved safety and cyclability by avoiding the need for a liquid electrolyte that could degrade.

3.4.4 Hybrid Li-Ion/Li–O₂ Insertion Electrodes

A novel type of Li–O₂ battery has been suggested in which both Li and O are accommodated into a transition metal oxide host [132, 133]. This has been referred to as a ‘hybrid’ Li-ion/Li–O₂ battery because it contains elements of both chemistries: Li⁺ ion insertion into a host as well as the reduction of oxygen. One example of this chemistry is the reaction $\text{LiFeO}_2 + 4\text{Li}^+ + 4\text{e}^- + \text{O}_2 \rightarrow \text{Li}_5\text{FeO}_4$, which can be thought of as the addition of Li₂O to Fe₂O₃. Although the presence of the transition metal oxide lowers the maximum theoretical energy density compared to a ‘traditional’ Li–O₂ battery that forms Li₂O₂, some hybrid Li-ion/Li–O₂ chemistries have been predicted to have an energy density competitive with Li₂O₂. A recent high-throughput computational study identified several candidate hybrid Li-ion/Li–O₂ chemistries based on capacity, voltage, and band gap [134].

3.4.5 Other Concepts

Metal-oxygen batteries bear a resemblance to some biological systems, where the reduction of oxygen is used as an energy source. Some of the challenges of non-aqueous Li–O₂ batteries have also been encountered by nature, including ‘oxidative stress’ (deleterious reactions involving reactive species such as superoxide radicals, peroxides, and singlet oxygen [135]) and the sluggish transport of O₂ in fluids.

Nature’s solutions to these challenges may inspire improvements in Li–O₂ cell design. For example, biological systems mitigate oxidative stress by antioxidants: molecules that scavenge reactive species [136]. One study applied this concept to Li–O₂ cells, and found that synthetic melanin additives led to improved cyclability [137]. Oxygen transport limitations are addressed in nature via the use of oxygen-binding proteins (e.g., hemoglobin) that improve O₂ solubility and also forced convection through the cardiovascular system [135]. These concepts can be applied to Li–O₂ cells: one study found that oxygen-binding perfluorinated additives improved discharge capacity [138]. No reports, to the best of our knowledge, have employed forced convection in Li–O₂ cells; however, continuum-scale models have predicted that the use of forced convection could significantly improve Li–O₂ discharge capacity [139].

Other approaches for improving oxygen transport in Li–O₂ cells have also been explored. The conceptually simplest approach is simply to increase the partial pressure of oxygen gas, which has been demonstrated to increase capacity significantly [140, 141]. Another concept for improving oxygen transport is the use of two immiscible liquids: one that facilitates Li-ion transport, and another that facilitates oxygen transport. A recent study demonstrated that the use of perfluorinated carbon liquids in this manner can significantly improve the capacity of Li–O₂ cells [142]. A similar concept is the use of additives to improve the solubility of Li₂O₂ and reaction intermediates [143].

4 Other Metal-Oxygen Chemistries

At this point our discussion has focused primarily on the Li–O₂ system, as among non-aqueous metal-oxygen chemistries, this system has received by far the most attention in the literature. A few recent studies, however, have begun to examine secondary room-temperature non-aqueous systems based on other alkali and alkaline-earth metals such as sodium [144–146], potassium [147], magnesium [148, 149], and aluminum [150], as shown in Table 2. The high abundance of these elements is often provided as a motivation for these systems, although projections indicate that the worldwide supply of Li is adequate for the next century [151]. Below we discuss some other potential advantages and disadvantages of these systems compared to Li–O₂.

Although necessarily sacrificing some gravimetric performance, the heavier Na- and K-based systems are noteworthy for two reasons: First, under some operating conditions, they appear to form a superoxide (NaO₂ or KO₂) discharge product, rather than peroxide. Second, the overpotentials observed during charging of these superoxides are very small in comparison to those for Li₂O₂ or Na₂O₂. One may therefore argue that what these cells lack in specific capacity is partially compensated for by an increase in voltaic efficiency. More importantly, if the formation of a superoxide discharge product is indeed responsible for higher efficiency, then a potential pathway for improving the Li–O₂ system may be at hand: by stabilizing a lithium superoxide (LiO₂) discharge phase one may realize high capacity and efficiency (i.e., low recharge overpotentials) simultaneously. However, such an approach may be challenging: although a superoxide component has been observed in the Li–O₂ discharge product, bulk LiO₂ is apparently unstable under ambient temperatures and pressures [152, 153]. The fact that NaO₂ and KO₂ are more stable than LiO₂ has been attributed to the smaller size of the Li⁺ cation [56].

In addition to alkali-metal-based systems, recent studies have recently reported secondary non-aqueous metal-oxygen cells using magnesium [148, 149] and aluminum [150] negative electrodes. These chemistries are noteworthy because the theoretical gravimetric and volumetric energy densities of cells that discharges to MgO or Al₂O₃ surpass the energy densities of a cell that discharges to Li₂O₂, Fig. 1.

However, further quantitative measurements will be required to definitively determine to what extent $\text{MgO}/\text{Al}_2\text{O}_3$ formation occurs in these cells. Furthermore, the challenges facing these systems appear to be even greater than for $\text{Li}-\text{O}_2$ because of the difficulties in finding electrolytes compatible with a Mg- or Al-metal negative electrode [154].

5 Concluding Remarks

Metal-oxygen batteries have been known for more than 150 years. Despite this long history, new twists on this well-known chemistry have continued to emerge up to the present day. Arguably the most exciting and rapid developments have occurred in only the past five years, coinciding with the demonstration of non-aqueous, reversible systems that in some cases exhibit extremely high energy densities in a laboratory setting. In particular, research into the $\text{Li}-\text{O}_2$ chemistry has progressed rapidly, and has been successful in pinpointing the primary challenges that must be overcome for a reversible $\text{Li}-\text{O}_2$ battery to become commercially viable. Key amongst these are: electrolyte stability, efficient transport (of oxygen within the electrolyte and electronic charge carriers within the discharge product), and implementing a high-capacity metal negative electrode. Although breakthroughs are needed in all three areas, a prudent strategy would be to focus first on realizing a reversible metal negative electrode. Such a technology could also be translated (perhaps with minimal additional development) to other, more mature systems such as those based on conventional Li-ion or lithium–sulfur technology, potentially ‘killing *several* birds with one stone.’ Success in this area will likely hinge upon development of a solid electrolyte capable of suppressing dendrite formation, while allowing for high ionic conductivity.

Should these cell-level challenges be overcome, another set of challenges for non-aqueous metal-oxygen batteries loom at the system level. These include the engineering of an efficient balance of plant that would either store oxygen on board (in a closed system), or separate it from an incoming flow of air (open system). Table 3 summarizes projected energy densities at the system level for an automotive scale $\text{Li}-\text{O}_2$ battery from three recent studies. While there is a wide range in the projected values, it is clear that the mass and volume associated with the system

Table 3 Projected system-level energy densities for non-aqueous $\text{Li}-\text{O}_2$ batteries

Institution	Gravimetric energy density (Wh/kg)	Volumetric energy density (Wh/L)
JCESR [26]	200–500	300–450
Bosch [15]	650–850	550–950
Ford [27]	640	600

incur a large penalty based on the much higher theoretical densities reported in Fig. 1. Minimizing these penalties will require novel engineering solutions.

Acknowledgments The authors gratefully acknowledge financial support from the U.S. National Science Foundation, grant no. CBET-1351482.

References

1. Vergnes M (1860) Improvement in the construction of voltaic gas-batteries. US Patent 28317
2. Shao Y, Ding F, Xiao J et al (2013) Making Li-air batteries rechargeable: material challenges. *Adv Funct Mater* 23:987–1004. doi:[10.1002/adfm.201200688](https://doi.org/10.1002/adfm.201200688)
3. Heise GW, Schumacher EA (1932) An air-depolarized primary cell with caustic alkali electrolyte. *J Electrochem Soc* 62:383–391. doi:[10.1149/1.3493794](https://doi.org/10.1149/1.3493794)
4. Reddy TB, Linden D (2011) *Handbook of batteries*. McGraw-Hill Companies, New York
5. Moehlenbrock MJ, Minteer SD (2008) Extended lifetime biofuel cells. *Chem Soc Rev* 37:1188–1196. doi:[10.1039/b708013c](https://doi.org/10.1039/b708013c)
6. Srinivasan S (2006) *Fuel cells: from fundamentals to applications*. Springer, New York
7. Yu X, Pickup PG (2008) Recent advances in direct formic acid fuel cells (DFAFC). *J Power Sources* 182:124–132. doi:[10.1016/j.jpowsour.2008.03.075](https://doi.org/10.1016/j.jpowsour.2008.03.075)
8. Ma J, Choudhury NA, Sahai Y (2010) A comprehensive review of direct borohydride fuel cells. *Renew Sustain Energy Rev* 14:183–199. doi:[10.1016/j.rser.2009.08.002](https://doi.org/10.1016/j.rser.2009.08.002)
9. Abraham KM, Jiang Z (1996) A polymer electrolyte-based rechargeable lithium/oxygen battery. *J Electrochem Soc* 143:1–5. doi:[10.1149/1.1836378](https://doi.org/10.1149/1.1836378)
10. Toni JEA, McDonald GD, Elliott WE (1966) Lithium-moist air battery. Fort Belvoir, Virginia
11. Blurton KF, Sammells AF (1979) Metal/air review batteries: their status and potential—a review. *J Power Sources* 4:263–279. doi:[10.1016/0378-7753\(79\)80001-4](https://doi.org/10.1016/0378-7753(79)80001-4)
12. Semkow KW, Sammells AF (1987) A lithium oxygen secondary battery. *J Electrochem Soc* 134:2084–2085. doi:[10.1149/1.2100826](https://doi.org/10.1149/1.2100826)
13. Abraham KM (2008) A brief history of non-aqueous metal-air batteries. *ECS Trans* 3:67–71. doi:[10.1149/1.2838193](https://doi.org/10.1149/1.2838193)
14. Zhang T, Zhou H (2013) A reversible long-life lithium-air battery in ambient air. *Nat Commun* 4:1817. doi:[10.1038/ncomms2855](https://doi.org/10.1038/ncomms2855)
15. Imanishi N, Luntz AC, Bruce P (2014) *The lithium air battery: fundamentals*. Springer, Berlin
16. Lu J, Li L, Park J-B et al (2014) Aprotic and aqueous Li–O₂ batteries. *Chem Rev* 114:5611–5640. doi:[10.1021/cr400573b](https://doi.org/10.1021/cr400573b)
17. Wang J, Li Y, Sun X (2013) Challenges and opportunities of nanostructured materials for aprotic rechargeable lithium–oxygen batteries. *Nano Energy* 2:443–467. doi:[10.1016/j.nanoen.2012.11.014](https://doi.org/10.1016/j.nanoen.2012.11.014)
18. Li Q, Cao R, Cho J, Wu G (2014) Nanostructured carbon-based cathode catalysts for nonaqueous lithium–oxygen batteries. *Phys Chem Chem Phys*. doi:[10.1039/C4CP00225C](https://doi.org/10.1039/C4CP00225C)
19. Balaish M, Kraysberg A, Ein-Eli Y (2014) A critical review on lithium-air battery electrolytes. *Phys Chem Chem Phys* 16:2801–2822. doi:[10.1039/c3cp54165g](https://doi.org/10.1039/c3cp54165g)
20. Yuan J, Yu J-S, Sundén B (2015) Review on mechanisms and continuum models of multi-phase transport phenomena in porous structures of non-aqueous Li-Air batteries. *J Power Sources* 278:352–369. doi:[10.1016/j.jpowsour.2014.12.078](https://doi.org/10.1016/j.jpowsour.2014.12.078)
21. Guo Z, Dong X, Yuan S et al (2014) Humidity effect on electrochemical performance of Li–O₂ batteries. *J Power Sources* 264:1–7. doi:[10.1016/j.jpowsour.2014.04.079](https://doi.org/10.1016/j.jpowsour.2014.04.079)

22. Trahan MJ, Mukerjee S, Plichta EJ et al (2012) Studies of Li-air cells utilizing dimethyl sulfoxide-based electrolyte. *J Electrochem Soc* 160:A259–A267. doi:[10.1149/2.048302jes](https://doi.org/10.1149/2.048302jes)
23. Adams BD, Radtke C, Black R et al (2013) Current density dependence of peroxide formation in the Li–O₂ battery and its effect on charge. *Energy Environ Sci* 6:1772. doi:[10.1039/c3ee40697k](https://doi.org/10.1039/c3ee40697k)
24. Geaney H, O’Connell J, Holmes JD, O’Dwyer C (2014) On the use of gas diffusion layers as current collectors in Li–O₂ battery cathodes. *J Electrochem Soc* 161:A1964–A1968. doi:[10.1149/2.0021414jes](https://doi.org/10.1149/2.0021414jes)
25. Houghton R, Gouty D, Allinson J et al (2012) Monitoring the location of cathode-reactions in Li–O₂ batteries. *J Electrochem Soc* 162:A3126–A3132. doi:[10.1149/2.0191502jes](https://doi.org/10.1149/2.0191502jes)
26. Gallagher KG, Goebel S, Greszler T et al (2014) Quantifying the promise of lithium–air batteries for electric vehicles. *Energy Environ Sci*. doi:[10.1039/c3ee43870h](https://doi.org/10.1039/c3ee43870h)
27. Adams J, Karulkar M (2012) Bipolar plate cell design for a lithium air battery. *J Power Sources* 199:247–255. doi:[10.1016/j.jpowsour.2011.10.041](https://doi.org/10.1016/j.jpowsour.2011.10.041)
28. Jung H-G, Hassoun J, Park J-B et al (2012) An improved high-performance lithium-air battery. *Nat Chem* 4:579–585. doi:[10.1038/nchem.1376](https://doi.org/10.1038/nchem.1376)
29. Mitchell RR, Gallant BM, Thompson CV, Shao-Horn Y (2011) All-carbon-nanofiber electrodes for high-energy rechargeable Li–O₂ batteries. *Energy Environ Sci* 4:2952–2958. doi:[10.1039/c1ee01496j](https://doi.org/10.1039/c1ee01496j)
30. Sun B, Huang X, Chen S et al (2014) Porous graphene nanoarchitectures: an efficient catalyst for low charge-overpotential, long life, and high capacity lithium–oxygen batteries. *Nano Lett* 14:3145–3152. doi:[10.1021/nl500397y](https://doi.org/10.1021/nl500397y)
31. Kwabi DG, Ortiz-Vitoriano N, Freunberger Sa et al (2014) Materials challenges in rechargeable lithium–air batteries. *MRS Bull* 39:443–452. doi:[10.1557/mrs.2014.87](https://doi.org/10.1557/mrs.2014.87)
32. Lu J, Lei Y, Lau KC et al (2013) A nanostructured cathode architecture for low charge overpotential in lithium–oxygen batteries. *Nat Commun* 4:2383. doi:[10.1038/ncomms3383](https://doi.org/10.1038/ncomms3383)
33. Yilmaz E, Yogi C, Yamanaka K et al (2013) Promoting formation of noncrystalline Li₂O₂ in Li–O₂ battery with RuO₂ nanoparticles. *Nano Lett* 13:4679–4684. doi:[10.1021/nl4020952](https://doi.org/10.1021/nl4020952)
34. Meini S, Piana M, Tsiouvaras N et al (2012) The effect of water on the discharge capacity of a non-catalyzed carbon cathode for Li–O₂ batteries. *Electrochem Solid-State Lett* 15:A45–A48. doi:[10.1149/2.005204esl](https://doi.org/10.1149/2.005204esl)
35. Meini S, Solchenbach S, Piana M, Gasteiger Ha (2014) The role of electrolyte solvent stability and electrolyte impurities in the electrooxidation of Li₂O₂ in Li–O₂ batteries. *J Electrochem Soc* 161:A1306–A1314. doi:[10.1149/2.0621409jes](https://doi.org/10.1149/2.0621409jes)
36. Aetukuri NB, McCloskey BD, García JM et al (2014) Solvating additives drive solution-mediated electrochemistry and enhance toroid growth in non-aqueous Li–O₂ batteries. *Nat Chem* 7:50–56. doi: [10.1038/nchem.2132](https://doi.org/10.1038/nchem.2132)
37. Mitchell RR, Gallant BM, Shao-Horn Y, Thompson CV (2013) Mechanisms of morphological evolution of Li₂O₂ particles during electrochemical growth. *J Phys Chem Lett* 4:1060–1064. doi:[10.1021/jz4003586](https://doi.org/10.1021/jz4003586)
38. Viswanathan V, Thygesen KS, Hummelshøj JS et al (2011) Electrical conductivity in Li₂O₂ and its role in determining capacity limitations in non-aqueous Li–O₂ batteries. *J Chem Phys* 135:214704. doi:[10.1063/1.3663385](https://doi.org/10.1063/1.3663385)
39. Griffith LD, Sleightholme AES, Mansfield JF et al (2015) Correlating Li/O₂ Cell Capacity and Product Morphology with Discharge Current. *ACS Appl Mater Interfaces* 7:7670–7678. doi:[10.1021/acsami.5b00574](https://doi.org/10.1021/acsami.5b00574)
40. Jung H-G, Kim H-S, Park J-B et al (2012) A transmission electron microscopy study of the electrochemical process of lithium–oxygen cells. *Nano Lett* 1:2–4. doi:[10.1021/nl302066d](https://doi.org/10.1021/nl302066d)
41. Zhai D, Wang H-H, Yang J et al (2013) Disproportionation in Li–O₂ batteries based on a large surface area carbon cathode. *J Am Chem Soc* 135:15364–15372. doi:[10.1021/ja403199d](https://doi.org/10.1021/ja403199d)
42. Xia C, Waletzko M, Peppler K, Janek J (2013) Silica nanoparticles as structural promoters for oxygen cathodes of lithium–oxygen batteries. *J Phys Chem C* 117:19897–19904. doi:[10.1021/jp407011d](https://doi.org/10.1021/jp407011d)

43. Xu J-J, Wang Z-L, Xu D et al (2013) Tailoring deposition and morphology of discharge products towards high-rate and long-life lithium–oxygen batteries. *Nat Commun* 4:2438. doi:[10.1038/ncomms3438](https://doi.org/10.1038/ncomms3438)
44. Lu J, Cheng L, Lau KC et al (2014) Effect of the size-selective silver clusters on lithium peroxide morphology in lithium–oxygen batteries. *Nat Commun* 5:4895. doi:[10.1038/ncomms5895](https://doi.org/10.1038/ncomms5895)
45. Xia C, Waletzko M, Chen L et al (2014) Evolution of Li₂O₂ growth and its effect on kinetics of Li–O₂ batteries. *ACS Appl Mater Interfaces* 6:12083–12092. doi:[10.1021/am5010943](https://doi.org/10.1021/am5010943)
46. Schwenke KU, Metzger M, Restle T et al (2015) The influence of water and protons on Li₂O₂ crystal growth in aprotic Li–O₂ cells. *J Electrochem Soc* 162:A573–A584. doi:[10.1149/2.0201504jes](https://doi.org/10.1149/2.0201504jes)
47. Aetukuri NB, McCloskey BD, García JM et al (2014) Solvating additives drive solution-mediated electrochemistry and enhance toroid growth in non-aqueous Li–O₂ batteries. *Nat Chem*. doi:[10.1038/nchem.2132](https://doi.org/10.1038/nchem.2132)
48. Kosma Va, Beltsios KG (2013) Simple solution routes for targeted carbonate phases and intricate carbonate and silicate morphologies. *Mater Sci Eng, C* 33:289–297. doi:[10.1016/j.msec.2012.08.042](https://doi.org/10.1016/j.msec.2012.08.042)
49. Felker FC, Kenar JA, Fanta GF, Biswas A (2013) Comparison of microwave processing and excess steam jet cooking for spherulite production from amylose–fatty acid inclusion complexes. *Starch* 65:864–874. doi:[10.1002/star.201200218](https://doi.org/10.1002/star.201200218)
50. Horstmann B, Gallant B, Mitchell R et al (2013) Rate-dependent morphology of Li₂O₂ growth in Li–O₂ batteries. *J Phys Chem Lett* 4:4217–4222
51. Morse JW, Casey WH (1988) Ostwald processes and mineral paragenesis in sediments. *Am J Sci* 288:537–560
52. Feenstra TP, De Bruyn PL (1981) The Ostwald rule of stages in precipitation from highly supersaturated solutions: a model and its application to the formation of the nonstoichiometric amorphous calcium phosphate precursor phase. *J Colloid Interface Sci* 84:66–72
53. Ostwald W (1897) Studien über die Umwandlung fester Körper. *Z Phys Chem* 22:289–330
54. Tian F, Radin MD, Siegel DJ (2014) Enhanced charge transport in amorphous Li₂O₂. *Chem Mater* 26:2952–2959. doi:[10.1021/cm5007372](https://doi.org/10.1021/cm5007372)
55. Lau KC, Lu J, Luo X et al (2014) Implications of the unpaired spins in Li–O₂ battery chemistry and electrochemistry: a minireview. *Chempluschem* 80:336–343. doi:[10.1002/cplu.201402053](https://doi.org/10.1002/cplu.201402053)
56. Vannerberg N-G (1962) Peroxides, superoxides, and ozonides of the metals of groups Ia, IIa, and IIb. *Prog Inorg Chem*. Wiley, Hoboken, pp 125–197
57. Lu J, Jung H-J, Lau KC et al (2013) Magnetism in lithium–oxygen discharge product. *ChemSusChem* 6:1196–1202. doi:[10.1002/cssc.201300223](https://doi.org/10.1002/cssc.201300223)
58. Radin MD, Rodriguez JF, Tian F, Siegel DJ (2012) Lithium peroxide surfaces are metallic, while lithium oxide surfaces are not. *J Am Chem Soc* 134:1093–1103. doi:[10.1021/ja208944x](https://doi.org/10.1021/ja208944x)
59. Ong SP, Mo Y, Ceder G (2012) Low hole polaron migration barrier in lithium peroxide. *Phys Rev B* 85:081105. doi:[10.1103/PhysRevB.85.081105](https://doi.org/10.1103/PhysRevB.85.081105)
60. Radin MD, Siegel DJ (2013) Charge transport in lithium peroxide: relevance for rechargeable metal–air batteries. *Energy Environ Sci* 6:2370–2379. doi:[10.1039/c3ee41632a](https://doi.org/10.1039/c3ee41632a)
61. Trahan MJ, Jia Q, Mukerjee S et al (2013) Cobalt phthalocyanine catalyzed lithium–air batteries. *J Electrochem Soc* 160:A1577–A1586. doi:[10.1149/2.118309jes](https://doi.org/10.1149/2.118309jes)
62. Thapa AK, Hidaka Y, Hagiwara H et al (2011) Mesoporous β-MnO₂ air electrode modified with Pd for rechargeability in lithium–air battery. *J Electrochem Soc* 158:A1483. doi:[10.1149/2.090112jes](https://doi.org/10.1149/2.090112jes)
63. Xu W, Xu K, Viswanathan VV et al (2011) Reaction mechanisms for the limited reversibility of Li–O₂ chemistry in organic carbonate electrolytes. *J Power Sources* 196:9631–9639. doi:[10.1016/j.jpowsour.2011.06.099](https://doi.org/10.1016/j.jpowsour.2011.06.099)

64. Meini S, Tsiouvaras N, Schwenke KU et al (2013) Rechargeability of Li–air cathodes pre-filled with discharge products using an ether-based electrolyte solution: implications for cycle-life of Li–air cells. *Phys Chem Chem Phys* 15:11478–11493. doi:[10.1039/c3cp51112j](https://doi.org/10.1039/c3cp51112j)
65. McCloskey BD, Valery A, Luntz AC et al (2013) Combining accurate O₂ and Li₂O₂ assays to separate discharge and charge stability limitations in nonaqueous Li–O₂ batteries. *J Phys Chem Lett* 4:2989–2993. doi:[10.1021/jz401659f](https://doi.org/10.1021/jz401659f)
66. Freunberger S, Chen Y, Drewett NE et al (2011) The lithium–oxygen battery with ether-based electrolytes. *Angew Chem Int Ed Engl* 50:8609–8613. doi:[10.1002/anie.201102357](https://doi.org/10.1002/anie.201102357)
67. Luntz AC, Viswanathan V, Voss J et al (2013) Tunneling and polaron charge transport through Li₂O₂ in Li–O₂ batteries. *J Phys Chem Lett* 4:3494–34997. doi:[10.1021/jz401926f](https://doi.org/10.1021/jz401926f)
68. Garcia-Lastra JM, Myrdal JSG, Christensen R et al (2013) DFT+U study of polaronic conduction in Li₂O₂ and Li₂CO₃: implications for Li–Air batteries. *J Phys Chem C* 117:5568–5577. doi:[10.1021/jp3107809](https://doi.org/10.1021/jp3107809)
69. Lu Y-C, Gallant BM, Kwabi DG et al (2013) Lithium–oxygen batteries: bridging mechanistic understanding and battery performance. *Energy Environ Sci* 6:750. doi:[10.1039/c3ee23966g](https://doi.org/10.1039/c3ee23966g)
70. Safari M, Adams BD, Nazar LF (2014) Kinetics of oxygen reduction in aprotic Li–O₂ cells: a model-based study. *J Phys Chem Lett* 5:3486–3491. doi:[10.1021/jz5018202](https://doi.org/10.1021/jz5018202)
71. Xue K, Mcturk E, Johnson L et al (2015) A comprehensive model for non-aqueous lithium air batteries involving different reaction mechanisms 162:614–621. doi:[10.1149/2.0121504jes](https://doi.org/10.1149/2.0121504jes)
72. Kang S, Mo Y, Ong SP, Ceder G (2013) A facile mechanism for recharging Li₂O₂ in Li–O₂ batteries. *Chem Mater* 25:3328–3336. doi:[10.1021/cm401720n](https://doi.org/10.1021/cm401720n)
73. Gallant BM, Kwabi DG, Mitchell RR et al (2013) Influence of Li₂O₂ morphology on oxygen reduction and evolution kinetics in Li–O₂ batteries. *Energy Environ Sci* 6:2518. doi:[10.1039/c3ee40998h](https://doi.org/10.1039/c3ee40998h)
74. Radin MD, Monroe CW, Siegel DJ (2015) How dopants can enhance charge transport in Li₂O₂. *Chem Mater* 27:839–847. doi:[10.1021/cm503874c](https://doi.org/10.1021/cm503874c)
75. Malik R, Abdellahi A, Ceder G (2013) A critical review of the Li insertion mechanisms in LiFePO₄ electrodes. *J Electrochem Soc* 160:A3179–A3197. doi:[10.1149/2.029305jes](https://doi.org/10.1149/2.029305jes)
76. Albertus P, Girishkumar G, McCloskey B et al (2011) Identifying capacity limitations in the Li/Oxygen battery using experiments and modeling. *J Electrochem Soc* 158:A343. doi:[10.1149/1.3527055](https://doi.org/10.1149/1.3527055)
77. Das SK, Xu S, Emwas A-H et al (2012) High energy lithium–oxygen batteries—transport barriers and thermodynamics. *Energy Environ Sci* 5:8927. doi:[10.1039/c2ee22470d](https://doi.org/10.1039/c2ee22470d)
78. Lu Y-C, Shao-Horn Y (2013) Probing the reaction kinetics of the charge reactions of nonaqueous Li–O₂ batteries. *J Phys Chem Lett* 4:93–99. doi:[10.1021/jz3018368](https://doi.org/10.1021/jz3018368)
79. Viswanathan V, Nørskov JK, Speidel A et al (2013) Li–O₂ kinetic overpotentials: Tafel plots from experiment and first-principles theory. *J Phys Chem Lett* 4:556–560. doi:[10.1021/jz400019y](https://doi.org/10.1021/jz400019y)
80. Gerbig O, Merkle R, Maier J (2013) Electron and ion transport in Li₂O₂. *Adv Mater* 25:3129–3133. doi:[10.1002/adma.201300264](https://doi.org/10.1002/adma.201300264)
81. Radin MD (2014) First-principles and continuum modeling of charge transport in Li–O₂ batteries. University of Michigan, Ann Arbor
82. Radin MD, Tian F, Siegel DJ (2012) Electronic structure of Li₂O₂ 0001 surfaces. *J Mater Sci* 47:7564–7570. doi:[10.1007/s10853-012-6552-6](https://doi.org/10.1007/s10853-012-6552-6)
83. Geng WT, He BL, Ohno T (2013) Grain boundary induced conductivity in Li₂O₂. *J Phys Chem C* 117:25222–25228. doi:[10.1021/jp405315k](https://doi.org/10.1021/jp405315k)
84. Zhao Y, Ban C, Kang J et al (2012) P-type doping of lithium peroxide with carbon sheets. *Appl Phys Lett* 101:023903. doi:[10.1063/1.4733480](https://doi.org/10.1063/1.4733480)
85. Zhu D, Zhang L, Song M et al (2013) Intermittent operation of the aprotic Li–O₂ battery: the mass recovery process upon discharge interval. *J Solid State Electrochem* 17:2539–2544. doi:[10.1007/s10008-013-2116-1](https://doi.org/10.1007/s10008-013-2116-1)

86. Sahapatsumbut U, Cheng H, Scott K (2013) Modelling the micro–macro homogeneous cycling behaviour of a lithium–air battery. *J Power Sources* 227:243–253. doi:[10.1016/j.jpowsour.2012.11.053](https://doi.org/10.1016/j.jpowsour.2012.11.053)
87. Nimon VY, Visco SJ, De Jonghe LC et al (2013) Modeling and experimental study of porous carbon cathodes in Li–O₂ cells with non-aqueous electrolyte. *ECS Electrochem Lett* 2:A33–A35. doi:[10.1149/2.004304eel](https://doi.org/10.1149/2.004304eel)
88. Liu J, Monroe CW (In preparation)
89. Chen XJ, Bevara VV, Andrei P et al (2014) Combined effects of oxygen diffusion and electronic resistance in Li–Air batteries with carbon nanofiber cathodes. *J Electrochem Soc* 161:A1877–A1883. doi:[10.1149/2.0721412jes](https://doi.org/10.1149/2.0721412jes)
90. Hummelshøj JS, Luntz AC, Nørskov JK (2013) Theoretical evidence for low kinetic overpotentials in Li–O₂ electrochemistry. *J Chem Phys* 138:034703. doi:[10.1063/1.4773242](https://doi.org/10.1063/1.4773242)
91. Mo Y, Ong S, Ceder G (2011) First-principles study of the oxygen evolution reaction of lithium peroxide in the lithium–air battery. *Phys Rev B* 84:205446. doi:[10.1103/PhysRevB.84.205446](https://doi.org/10.1103/PhysRevB.84.205446)
92. Lee B, Seo D-H, Lim H-D et al (2014) First-principles study of the reaction mechanism in sodium–oxygen batteries. *Chem Mater* 26:1048–1055. doi:[10.1021/cm403163c](https://doi.org/10.1021/cm403163c)
93. Leung K (2013) Electronic structure modeling of electrochemical reactions at electrode/electrolyte interfaces in lithium ion batteries. *J Phys Chem C* 117:1539–1547. doi:[10.1021/jp308929a](https://doi.org/10.1021/jp308929a)
94. Mizuno F, Nakanishi S, Kotani Y et al (2010) Rechargeable Li–Air batteries with carbonate-based liquid electrolytes. *Electrochemistry* 78:403–405
95. McCloskey B, Bethune D, Shelby R et al (2011) Solvents’ critical role in nonaqueous lithium–oxygen battery. *J Phys Chem Lett* 2:1161–1166
96. Laino T, Curioni A (2012) A new piece in the puzzle of lithium/air batteries: computational study on the chemical stability of propylene carbonate in the presence of lithium peroxide. *Chem—Eur J* 18:3510–3520. doi:[10.1002/chem.201103057](https://doi.org/10.1002/chem.201103057)
97. McCloskey BD, Bethune DS, Shelby RM et al (2012) Limitations in rechargeability of Li–O₂ batteries and possible origins. *J Phys Chem Lett* 3:3043–3047
98. Veith GM, Nanda J, Delmau LH, Dudney NJ (2012) Influence of lithium salts on the discharge chemistry of Li–Air cells. *J Phys Chem Lett* 3:1242–1247. doi:[10.1021/jz300430s](https://doi.org/10.1021/jz300430s)
99. Du P, Lu J, Lau KC et al (2013) Compatibility of lithium salts with solvent of the non-aqueous electrolyte in Li–O₂ batteries. *Phys Chem Chem Phys* 15:5572–5581. doi:[10.1039/c3cp50500f](https://doi.org/10.1039/c3cp50500f)
100. Younesi R, Hahlin M, Bjo F et al (2013) Li–O₂ battery degradation by lithium peroxide (Li₂O₂): a model study. *Chem Mater* 25:77–84. doi:[10.1021/cm303226g](https://doi.org/10.1021/cm303226g)
101. McCloskey BD, Speidel A, Scheffler R et al (2012) Twin problems of interfacial carbonate formation in nonaqueous Li–O₂ batteries. *J Phys Chem Lett* 3:997–1001. doi:[10.1021/jz300243r](https://doi.org/10.1021/jz300243r)
102. Ottakam Thotiyil MM, Freunberger SA, Peng Z, Bruce PG (2013) The carbon electrode in nonaqueous Li–O₂ cells. *J Am Chem Soc* 135:494–500. doi:[10.1021/ja310258x](https://doi.org/10.1021/ja310258x)
103. Nasybulin E, Xu W, Engelhard MH et al (2013) Stability of polymer binders in Li–O₂ batteries. *J Power Sources* 243:899–907. doi:[10.1016/j.jpowsour.2013.06.097](https://doi.org/10.1016/j.jpowsour.2013.06.097)
104. Shui J-L, Wang H-H, Liu D-J (2013) Degradation and revival of Li–O₂ battery cathode. *Electrochem Commun* 34:45–47. doi:[10.1016/j.elecom.2013.05.020](https://doi.org/10.1016/j.elecom.2013.05.020)
105. Peng Z, Freunberger SA, Chen Y, Bruce PG (2012) A reversible and higher-rate Li–O₂ battery. *Science* 80(337):563–566. doi:[10.1126/science.1223985](https://doi.org/10.1126/science.1223985)
106. Kar M, Simons TJ, Forsyth M, MacFarlane DR (2014) Ionic liquid electrolytes as a platform for rechargeable metal–air batteries: a perspective. *Phys Chem Chem Phys* 16:18658–18674. doi:[10.1039/C4CP02533D](https://doi.org/10.1039/C4CP02533D)
107. Lau KC, Lu J, Low J et al (2014) Investigation of the decomposition mechanism of lithium bis(oxalate)borate (LiBOB) salt in the electrolyte of an aprotic Li–O₂ battery. *Energy Technol* 2:348–354. doi:[10.1002/ente.201300164](https://doi.org/10.1002/ente.201300164)

108. Bryantsev V (2011) Computational study of the mechanisms of superoxide-induced decomposition of organic carbonate-based electrolytes. *J Phys Chem Lett* 2:379–383
109. Beyer H, Meini S, Tsiouvaras N et al (2013) Thermal and electrochemical decomposition of lithium peroxide in non-catalyzed carbon cathodes for Li–air batteries. *Phys Chem Chem Phys* 15:11025–11037. doi:[10.1039/c3cp51056e](https://doi.org/10.1039/c3cp51056e)
110. Bryantsev VS, Faglioni F (2012) Predicting autoxidation stability of ether- and amide-based electrolyte solvents for Li–air batteries. *J Phys Chem A* 116:7128–7138. doi:[10.1021/jp301537w](https://doi.org/10.1021/jp301537w)
111. Zhu D, Zhang L, Song M et al (2013) Solvent autoxidation, electrolyte decomposition, and performance deterioration of the aprotic Li–O₂ battery. *J Solid State Electrochem* 17:2865–2870. doi:[10.1007/s10008-013-2202-4](https://doi.org/10.1007/s10008-013-2202-4)
112. Assary RS, Lau KC, Amine K et al (2013) Interactions of dimethoxy ethane with Li₂O₂ clusters and likely decomposition mechanisms for Li–O₂ batteries. *J Phys Chem C* 117:8041–8049
113. Laino T, Curioni A (2013) Chemical reactivity of aprotic electrolytes on a solid Li₂O₂ surface: screening solvents for Li–air batteries. *New J Phys* 15:095009. doi:[10.1088/1367-2630/15/9/095009](https://doi.org/10.1088/1367-2630/15/9/095009)
114. McCloskey B, Scheffler R, Speidel A et al (2011) On the efficacy of electrocatalysis in nonaqueous Li–O₂ batteries. *J Am Chem Soc* 133:18038–18041
115. Harding JR, Lu Y, Shao-horn Y (2012) Evidence of catalyzed oxidation of Li₂O₂ for rechargeable Li–Air battery applications. *Phys Chem Chem Phys* 14:10540–10546. doi:[10.1039/c2cp41761h](https://doi.org/10.1039/c2cp41761h)
116. Cho MH, Trottier J, Gagnon C et al (2014) The effects of moisture contamination in the Li–O₂ battery. *J Power Sources* 268:565–574. doi:[10.1016/j.jpowsour.2014.05.148](https://doi.org/10.1016/j.jpowsour.2014.05.148)
117. Schwenke KU, Meini S, Wu X et al (2013) Stability of superoxide radicals in glyme solvents for non-aqueous Li–O₂ battery electrolytes. *Phys Chem Chem Phys* 15:11830–11839. doi:[10.1039/c3cp51531a](https://doi.org/10.1039/c3cp51531a)
118. Gowda SR, Brunet A, Wallraff GM, McCloskey BD (2013) Implications of CO₂ contamination in rechargeable nonaqueous Li–O₂ batteries. *J Phys Chem Lett* 4:276–279
119. Li F, Zhang T, Zhou H (2013) Challenges of non-aqueous Li–O₂ batteries: electrolytes, catalysts, and anodes. *Energy Environ Sci* 6:1125–1141. doi:[10.1039/c3ee00053b](https://doi.org/10.1039/c3ee00053b)
120. Xu W, Wang J, Ding F et al (2014) Lithium metal anodes for rechargeable batteries. *Energy Environ Sci* 7:513. doi:[10.1039/c3ee40795k](https://doi.org/10.1039/c3ee40795k)
121. Assary RS, Lu J, Du P et al (2012) The effect of oxygen crossover on the anode of a Li–O₂ battery using an ether-based solvent: insights from experimental and computational studies. *ChemSusChem* 6:51–55. doi:[10.1002/cssc.201200810](https://doi.org/10.1002/cssc.201200810)
122. Shui J-L, Okasinski JS, Kenesei P et al (2013) Reversibility of anodic lithium in rechargeable lithium-oxygen batteries. *Nat Commun* 4:2255. doi:[10.1038/ncomms3255](https://doi.org/10.1038/ncomms3255)
123. Roberts M, Younesi R, Richardson W et al (2014) Increased cycling efficiency of lithium anodes in dimethyl sulfoxide electrolytes for use in Li–O₂ batteries. *ECS Electrochem Lett* 3:A62–A65. doi:[10.1149/2.007406eel](https://doi.org/10.1149/2.007406eel)
124. Adams J, Karulkar M, Anandan V (2013) Evaluation and electrochemical analyses of cathodes for lithium-air batteries. *J Power Sources* 239:132–143. doi:[10.1016/j.jpowsour.2013.03.140](https://doi.org/10.1016/j.jpowsour.2013.03.140)
125. Yoon DH, Park YJ (2014) Characterization of real cyclic performance of air electrode for Li–Air batteries. *J Electroceram*. doi:[10.1007/s10832-014-9937-x](https://doi.org/10.1007/s10832-014-9937-x)
126. Ottakam Thotiyil MM, Freunberger SA, Peng Z et al (2013) A stable cathode for the aprotic Li–O₂ battery. *Nat Mater* 12:1–7. doi:[10.1038/nmat3737](https://doi.org/10.1038/nmat3737)
127. Chen Y, Freunberger SA, Peng Z et al (2013) Charging a Li–O₂ battery using a redox mediator. *Nat Chem* 5:489–494. doi:[10.1038/NCHEM.1646](https://doi.org/10.1038/NCHEM.1646)
128. Tan P, Shyy W, An L et al (2014) A gradient porous cathode for non-aqueous lithium–air batteries leading to a high capacity. *Electrochem Commun* 46:111–114. doi:[10.1016/j.elecom.2014.06.026](https://doi.org/10.1016/j.elecom.2014.06.026)

129. Black R, Lee J-H, Adams B et al (2013) The role of catalysts and peroxide oxidation in lithium-oxygen batteries. *Angew Chem Int Ed Engl* 52:392–396. doi:[10.1002/anie.201205354](https://doi.org/10.1002/anie.201205354)
130. Kim DS, Park YJ (2014) Effect of multi-catalysts on rechargeable Li–Air batteries. *J Alloys Compd* 591:164–169. doi:[10.1016/j.jallcom.2013.12.208](https://doi.org/10.1016/j.jallcom.2013.12.208)
131. Li F, Kitaura H, Zhou H (2013) The pursuit of rechargeable solid-state Li–Air batteries. *Energy Environ Sci* 6:2302. doi:[10.1039/c3ee40702k](https://doi.org/10.1039/c3ee40702k)
132. Thackeray MM, Chan MKY, Trahey L et al (2013) Vision for designing high-energy, hybrid Li Ion/Li–O₂ cells. *J Phys Chem Lett* 4:3607–3611
133. Trahey L, Karan NK, Chan MKY et al (2012) Synthesis, characterization, and structural modeling of high-capacity, dual functioning MnO₂ electrode/electrocatalysts for Li–O₂ cells. *Adv Energy Mater* 3:75–84. doi:[10.1002/aenm.201200037](https://doi.org/10.1002/aenm.201200037)
134. Kirklin S, Chan M, Trahey L et al (2014) High-throughput screening of high-capacity electrodes for hybrid Li-ion/Li–O₂ cells. *Phys Chem Chem Phys* 16:22073–22082. doi:[10.1039/C4CP03597F](https://doi.org/10.1039/C4CP03597F)
135. Popel AS (1989) Theory of oxygen transport to tissue. *Crit Rev Bioeng* 17:257–321
136. Kohen R, Nyska A (2002) Oxidation of biological systems: oxidative stress phenomena, antioxidants, redox reactions, and methods for their quantification. *Toxicol Pathol* 30:620–650. doi:[10.1080/0192623029016672](https://doi.org/10.1080/0192623029016672)
137. Kim BG, Kim S, Lee H, Choi JW (2014) Wisdom from the human eye: a synthetic melanin radical scavenger for improved cycle life of Li–O₂ battery. *Chem Mater* 26:4757–4764
138. Wang Y, Zheng D, Yang X-Q, Qu D (2011) High rate oxygen reduction in non-aqueous electrolytes with the addition of perfluorinated additives. *Energy Environ Sci* 4:3697. doi:[10.1039/c1ee01556g](https://doi.org/10.1039/c1ee01556g)
139. Li XL, Huang J, Faghri A (2014) Modeling study of a Li–Air battery with an active cathode. *Energy* 1–12. doi:[10.1016/j.energy.2014.12.062](https://doi.org/10.1016/j.energy.2014.12.062)
140. Nemanick EJ, Hickey RP (2014) The effects of O₂ pressure on Li–O₂ secondary battery discharge capacity and rate capability. *J Power Sources* 252:248–251. doi:[10.1016/j.jpowsour.2013.12.016](https://doi.org/10.1016/j.jpowsour.2013.12.016)
141. Zhang Y, Zhang H, Li J et al (2013) The use of mixed carbon materials with improved oxygen transport in a lithium–air battery. *J Power Sources* 240:390–396. doi:[10.1016/j.jpowsour.2013.04.018](https://doi.org/10.1016/j.jpowsour.2013.04.018)
142. Balaish M, Kraysberg A, Ein-Eli Y (2013) Realization of an artificial three-phase reaction zone in a Li–Air battery. *ChemElectroChem* n/a–n/a. doi:[10.1002/celec.201300055](https://doi.org/10.1002/celec.201300055)
143. Li C, Fontaine O, Freunberger SA et al (2014) Aprotic Li–O₂ battery: influence of complexing agents on oxygen reduction in an aprotic solvent. *J Phys Chem C* 118:3393–3401. doi:[10.1021/jp4093805](https://doi.org/10.1021/jp4093805)
144. Hartmann P, Bender CL, Vračar M et al (2013) A rechargeable room-temperature sodium superoxide (NaO₂) battery. *Nat Mater* 12:228–232. doi:[10.1038/nmat3486](https://doi.org/10.1038/nmat3486)
145. Ha S, Kim J-K, Choi A et al (2014) Sodium-metal halide and sodium-air batteries. *ChemPhysChem* 15:1971–1982. doi:[10.1002/cphc.201402215](https://doi.org/10.1002/cphc.201402215)
146. Liu W, Sun Q, Yang Y et al (2013) An enhanced electrochemical performance of a sodium-air battery with graphene nanosheets as air electrode catalysts. *Chem Comm* 49:1951–1953. doi:[10.1039/c3cc00085k](https://doi.org/10.1039/c3cc00085k)
147. Ren X, Wu Y (2013) A low-overpotential potassium-oxygen battery based on potassium superoxide. *J Am Chem Soc* 135:2923–2926. doi:[10.1021/ja312059q](https://doi.org/10.1021/ja312059q)
148. Shiga T, Hase Y, Yagi Y et al (2014) Catalytic cycle employing a TEMPO—anion complex to obtain a secondary Mg–O₂ battery. *J Phys Chem Lett* 5:1648–1652. doi:[10.1021/jz500602r](https://doi.org/10.1021/jz500602r)
149. Shiga T, Hase Y, Kato Y et al (2013) A rechargeable non-aqueous Mg–O₂ battery. *Chem Commun (Camb)* 49:9152–9154. doi:[10.1039/c3cc43477j](https://doi.org/10.1039/c3cc43477j)
150. Revel R, Audichon T, Gonzalez S (2014) Non-aqueous aluminium-air battery based on ionic liquid electrolyte. *J Power Sources* 272:415–421. doi:[10.1016/j.jpowsour.2014.08.056](https://doi.org/10.1016/j.jpowsour.2014.08.056)

151. Gruber PW, Medina PA, Keoleian GA et al (2011) Global lithium availability: a constraint for electric vehicles? *J Ind Ecol* 15:760–775. doi:[10.1111/j.1530-9290.2011.00359.x](https://doi.org/10.1111/j.1530-9290.2011.00359.x)
152. Sangster J, Pelton A (1992) The Li–O (lithium–oxygen) system. *J Phase Equilibria* 13:296–299
153. Lau KC, Curtiss LA, Greeley J (2011) Density functional investigation of the thermodynamic stability of lithium oxide bulk crystalline structures as a function of oxygen pressure. *J Phys Chem C* 115:23625–23633. doi:[10.1021/jp206796h](https://doi.org/10.1021/jp206796h)
154. Muldoon J, Bucur CB, Gregory T (2014) Quest for nonaqueous multivalent secondary batteries: magnesium and beyond. *Chem Rev* 114:11683–11720. doi:[10.1021/cr500049y](https://doi.org/10.1021/cr500049y)
155. Lu YC, Kwabi DG, Yao KPC et al (2011) The discharge rate capability of rechargeable Li–O₂ batteries. *Energy Environ Sci* 4:2999–3007. doi:[10.1039/c1ee01500a](https://doi.org/10.1039/c1ee01500a)
156. Kim BG, Kim H-J, Back S et al (2014) Improved reversibility in lithium–oxygen battery: understanding elementary reactions and surface charge engineering of metal alloy catalyst. *Sci Rep* 4:4225. doi:[10.1038/srep04225](https://doi.org/10.1038/srep04225)
157. Hayashi K, Shima K, Sugiyama F (2013) A mixed aqueous/aprotic sodium/air cell using a NASICON ceramic separator. *J Electrochem Soc* 160:A1467–A1472. doi:[10.1149/2.067309jes](https://doi.org/10.1149/2.067309jes)
158. Downing BW (2012) Metal–air technology. *Electrochem Technol Energy Storage Convers.* doi:[10.1002/9783527639496.ch6](https://doi.org/10.1002/9783527639496.ch6)
159. Cooper JF (1977) High performance metal/air fuel cells. OSTI ID: 7084912. doi:[10.2172/7084912](https://doi.org/10.2172/7084912)
160. Hosseiny SS, Saakes M, Wessling M (2011) A polyelectrolyte membrane-based vanadium/air redox flow battery. *Electrochem Commun* 13:751–754. doi:[10.1016/j.elecom.2010.11.025](https://doi.org/10.1016/j.elecom.2010.11.025)
161. Walker CW, Walker J (2012) Molybdenum/air battery and cell design. 2: US Patent 8148020 B2
162. Wagner OC (1969) Secondary cadmium–air cells. *J Electrochem Soc* 116:693. doi:[10.1149/1.2412023](https://doi.org/10.1149/1.2412023)
163. Egan DR, Ponce de León C, Wood RJK et al (2013) Developments in electrode materials and electrolytes for aluminium–air batteries. *J Power Sources* 236:293–310. doi:[10.1016/j.jpowsour.2013.01.141](https://doi.org/10.1016/j.jpowsour.2013.01.141)
164. Mori R (2014) A novel aluminium–air secondary battery with long-term stability. *RSC Adv* 4:1982. doi:[10.1039/c3ra44659j](https://doi.org/10.1039/c3ra44659j)
165. Zhong X, Zhang H, Liu Y et al (2012) High-capacity silicon–air battery in alkaline solution. *ChemSusChem* 5:177–180. doi:[10.1002/cssc.201100426](https://doi.org/10.1002/cssc.201100426)
166. Jiang R (2007) Combinatorial electrochemical cell array for high throughput screening of micro-fuel-cells and metal/air batteries. *Rev Sci Instrum* 78:072209. doi:[10.1063/1.2755439](https://doi.org/10.1063/1.2755439)
167. Inoishi A, Ju Y-W, Ida S, Ishihara T (2013) Mg–air oxygen shuttle batteries using a ZrO₂-based oxide ion-conducting electrolyte. *Chem Commun (Camb)* 49:4691–4693. doi:[10.1039/c3cc40880a](https://doi.org/10.1039/c3cc40880a)
168. Pujare NU, Semkow KW, Sammells AF (1988) A calcium oxygen secondary battery. *J Electrochem Soc* 135:260–261. doi:[10.1149/1.2095574](https://doi.org/10.1149/1.2095574)
169. Zhao X, Gong Y, Li X et al (2013) A new solid oxide molybdenum–air redox battery. *J Mater Chem A* 1:14858. doi:[10.1039/c3ta12726e](https://doi.org/10.1039/c3ta12726e)
170. Zhao X, Li X, Gong Y et al (2013) A high energy density all solid-state tungsten–air battery. *Chem Commun (Camb)* 49:5357–5359. doi:[10.1039/c3cc42075b](https://doi.org/10.1039/c3cc42075b)
171. Zhao X, Li X, Gong Y et al (2014) A novel intermediate-temperature all ceramic iron–air redox battery: the effect of current density and cycle duration. *RSC Adv* 4:22621. doi:[10.1039/c4ra02768j](https://doi.org/10.1039/c4ra02768j)
172. Desclaux P, Nürnberger S, Stimming U (2010) Direct carbon fuel cells. In: Steinberge-Wilckens R, Lehnert W (eds) *Innovations in fuel cell technologies*. The Royal Society of Chemistry, Cambridge, p 190–211 doi:[10.1039/9781849732109-00190](https://doi.org/10.1039/9781849732109-00190)
173. Cohn G, Starosvetsky D, Hagiwara R et al (2009) Silicon–air batteries. *Electrochem Commun* 11:1916–1918. doi:[10.1016/j.elecom.2009.08.015](https://doi.org/10.1016/j.elecom.2009.08.015)